COMPDYN 2011
III ECCOMAS Thematic Conference on
Computational Methods in Structural Dynamics and Earthquake Engineering
M. Papadrakakis, M. Fragiadakis, V. Plevris (eds.)
Corfu, Greece, 26-28 May 2011

SEISMIC STRENGTH EVALUATION OF REINFORCED CONCRETE SHEAR WALLS WITH CRACKS, USING THE NOTION OF FRACTAL GEOMETRY

O. Panagouli, E. Mistakidis and K. Iordanidou

Laboratory of Structural Analysis and Design, Dept. of Civil Engineering, University of Thessaly,
Pedion Areos, 38334 Volos, Greece
{olpanag,emistaki}@uth.gr

Keywords: Cracked shear walls, rough interfaces, fractal geometry, fractal resolution, unilateral contact, variational formulation

Abstract. *Shear walls play an important role to the seismic strength of modern seismic resistant structures. They are designed so that they have significant bending and shear strengths and ductility. However, existing structures have lightly reinforced shear walls. In most cases, especially under cycling loading, shear cracks appear reducing the shear capacity of the wall. Here, a typical shear wall of an existing structure is examined in which it is assumed that a crack has been formed. For the modeling of the geometry of the crack a new approach is applied, using the notion of fractal geometry. The aim of the paper is the estimation of the post-cracking strength of the wall, taking into account the geometry of the cracks and the mixed friction-plastification mechanisms that develop in the vicinity of the crack. Due to the significance of the crack geometry a multi-resolution analysis is performed. The materials (steel and concrete) are assumed to have elastic-plastic behaviour. For concrete both cracking and crushing are taken into account in an accurate manner. On the interface unilateral contact and friction conditions are assumed to hold. For every structure resulting for each resolution of the interface, a classical Euclidean problem is solved. The obtained results lead to interesting conclusions concerning the post-cracking strength of lightly reinforced shear walls.*

1 INTRODUCTION

Shear walls play a significant role to the seismic strength of structures built in seismic prone areas. Shear walls in modern structures are designed to have significant bending and shear strengths and ductility. However, shear walls in old, existing buildings have been constructed using poor materials and usually have inadequate shear strength. In such elements, shear cracks appear reducing their overall capacity. The aim of this paper is to apply, a new approach in order to estimate the post-cracking strength of a shear wall which is part of an existing structure, taking into account the geometry of the formed cracks. To this end, the notion of fractal geometry is applied in order to approximate the geometry of the crack.

It is well known that the geometry and structure of the interface between two solid surfaces in contact is of fundamental importance to the study of friction, wear, lubrication and also strength evaluation. Experimental studies [1], [2], [3], [4] have shown that the fracture interfaces have irregularities of all scales, and require advanced mathematical models for their description. In general, the actual contact between two real interfaces is realized only over a small fraction in a discrete number of areas. Consequently, the real area of contact is only a fraction of the apparent area [5], [6] and the parameters of the actual contact regions are strongly influenced by the roughness of the contacting surfaces. For that, fractal contact models are suitable for the simulation of contact.

The fractal approach adopted here for the simulation of the geometry of the cracks formed in the shear wall, uses computer generated self-affine curves for the modelling of the interface roughness, which is strongly dependent on the values of the structural parameters of these curves. The computer generated interfaces, which are characterized by a precise value of the resolution δ of the fractal curve, permit the study of the interface roughness on iteratively generated rough profiles. This fact makes this approach suitable for engineering problems, since it permits the satisfactory study of the whole problem with reliable numerical calculations.

Among the aims of this paper is to study how the resolution of a fractal interface F affects the strength of a reinforced concrete shear wall element, in which it is assumed that a crack has been developed. The geometry of the crack is modelled through the application of the principles of fractal geometry. On the interface between the two cracked surfaces, unilateral contact and friction conditions are assumed to hold. The applied approach takes into account the nonlinear behaviour of the materials, including the limited strength of the concrete under tension. The shear wall is applied to shear loading. As a result of the applied approach, the contribution of the friction between the cracked surfaces is taken into account, as well as the additional strength coming from the mechanical interlock between the two faces of the crack. For every structure resulting for each resolution of the interface, a classical Euclidean problem is solved by using a variational formulation [7].

2 FRACTAL REPRESENTATION OF ROUGH INTERFACES

The fractal nature of material damage has been a matter of a very intense research during the last three decades. The fractal nature of fracture surfaces in metals was shown more than 20 years ago by Mandelbrot et. al. [1]. In this paper the authors studied the fracture of cracked surfaces in metals fractured either by tensile or impact loading, which were shown to develop fractal structure over more than three orders of magnitude. In quasi-brittle materials observations have shown that fracture surfaces display self-affine scale properties in a certain range of scales which is in most cases very large and which greatly depends on the material micro-

structure. This is true for a large variety of quasi-brittle materials such as rock, concrete, wood and ceramics [8], [9].

Fractal sets are characterized by non-integer dimensions [10]. The dimension of a fractal set in plane can vary from 0 to 2. Accordingly, by increasing the resolution of a fractal set, its length tends to 0 if its dimension is smaller than 1 (totally disconnected set), or tends to infinity if it is larger than 1. In these cases the length is a nominal, useless quantity, since it changes as the resolution increases. Conversely, the fractal dimension of a fractal set is a parameter of great importance because of its scale-independent character.

Many methods which are based on experimental or numerical calculations, such as the Richardson method [10], have been developed for the estimation of the fractal dimension of a curve. According to this method, dividers, which are set to a prescribed opening δ, are used. Moving with these dividers along the curve so that each new step starts where the previous step leaves off, one obtains the number of steps $N(\delta)$. The curve is said to be of fractal nature if by repeating this procedure for different values of δ the relation

$$N(\delta) \sim \delta^{-D} \tag{1}$$

is obtained in some interval $\delta^{(*)} < \delta < \Delta^{(*)}$. The power D denotes the fractal dimension of the profile, which is in the range $1 \le D < 2$. The relation between the fractal dimension D of this profile and the dimension of the corresponding surface is $D_s = D + 1$ [10].

The idea of self-affinity is very popular in studying surface roughness because experimental studies have shown that usually, under repeated magnifications, the profiles of real surfaces are statistically self-affine to themselves [1], [11]. The self-affine fractals were used in a number of papers as a tool for the description of rough surfaces [12]-[17]. Typically, such a profile can be measured by taking height data y_i with respect to an arbitrary datum at N equidistant discrete points x_i and following the procedure presented in [18]. Here, fractal interpolation functions are used for the passage from this discrete set of data $\{(x_i, y_i), i = 0,1,2,...,N\}$ to a continuous model, where $\mathrm{F}(x_i) = y_i$, $i = 0,1,...,N$. It has been proved [18] that there is a sequence of functions $\mathrm{F}_{n+1}(x) = (T\mathrm{F}_n)(x)$, where $T : C^0 \to C^0$ is an operator defined by:

$$\mathrm{F}_{n+1}(x) = (T\mathrm{F}_n)(x) = c_i l_i^{-1}(x) + d_i \mathrm{F}_n\left(l_i^{-1}(x)\right) + g_i \tag{2}$$

for $x \in [x_{i-1}, x_i], i = 1,2,...,N$. The operator T converges to a fractal curve F , as $n \to \infty$. The transformation l_i transforms $[x_0, x_N]$ to $[x_{i-1}, x_i]$ and it is defined by the relation

$$l_i(x) = a_i x + b_i. \tag{3}$$

The factors d_i are the hidden variables of the transformations and they have to satisfy $0 \le d_i < 1$ in order for $T : C^0 \to C^0$ to have a unique fixed point. Moreover, the remaining parameters are given by the following equations:

$$a_i = (x_i - x_{i-1}) / (x_N - x_0) \tag{4}$$

$$c_i = (y_i - y_{i-1}) / (x_N - x_0) - d_i (y_N - y_0) / (x_N - x_0) \tag{5}$$

$$b_i = (x_N x_{i-1} - x_0 x_i) / (x_N - x_0) \tag{6}$$

$$g_i = \left(x_N y_{i-1} - x_0 y_i\right)/\left(x_N - x_0\right) - d_i\left(x_N y_0 - x_0 y_N\right)/\left(x_N - x_0\right). \tag{7}$$

The fractal interpolation functions give profiles which look quite attractive from the viewpoint of a graphic roughness simulation. In higher approximations these profiles appear rougher as it is shown in the next section where the first to fourth approximations of a fractal interpolation function are presented. Moreover, the roughness of the profile is strongly affected by the free parameters $d_i, i = 1,...,N$ of the interpolation functions. As these parameters take larger values, the resulting profiles appear rougher.

It must be mentioned here that an important advantage of the fractal interpolation functions presented here is that their fractal dimension can be obtained numerically [18] and is given by the relation:

$$\delta^{-D} \approx \sum_{i=1}^{N} |\, d_i \,|\, a_i^{D-1} \delta^{-D} \Leftrightarrow \sum_{i=1}^{N} |\, d_i \,| a_i^{D-1} = 1. \tag{8}$$

3 DESCRIPTION OF THE CONSIDERED PROBLEM

In Figure 1 a reinforced concrete shear wall element is presented which is assumed to be part of a typical existing structure built during the 60s or 70s. The wall is reinforced by a double steel mesh consisting of horizontal and vertical rebars having a diameter of 8mm and a spacing of 200mm. The quality of the steel mesh is assumed to be S220 (typical for buildings of that age). At the two ends of the wall the amount of reinforcement is higher. Four 20mm rebars of higher quality (S400) are used, without specific provisions to increase the confinement. The thickness of the wall is 200mm and the quality of concrete is assumed to be C16, typical for this kind of constructions. The wall is fixed on the lower horizontal boundary.

The considered shear wall is divided into two parts by a crack which is assumed that has been formed as a result of the action of an earthquake. Obviously, the depicted crack has been formed due to shear failure of concrete. For the description of the geometry of the crack, the notion of fractals is used. More specifically, the crack is assumed to be a fractal interface, described by the fixed point of a fractal interpolation function interpolating the set of data $\{(-1.0, 2.95), (0.4, 2.0)(1.8, 1.0)(3.2, 0.5)\}$. The free parameters of the fractal interpolation function are taken to have the values $d_1 = d_2 = d_3 = 0.50$.

The objective here is to estimate the capacity of the shear wall under an action similar to the one that has created the crack. For this reason, a horizontal displacement of 20mm is applied on the upper side of the wall (see Fig. 1). Moreover, a vertical distributed loading q_N is applied on the upper horizontal boundary, creating a compressive axial loading. The resultant of this loading is denoted by N. For N, six different values will be considered from 0 to 2.500 kN with a step of 500 kN.

As it was mentioned in the previous section, self-affine interfaces are adopted for the interface simulation. The computer generated interfaces $\mathrm{F}_n, n = 1, 2, ...$ are only images "pre-fractals" characterized by a precise value of the resolution $\delta^{(n)}$ of the fractal set. The resolution $\delta^{(n)}$ is related to the (n)-th iteration of the fractal interpolation function and represents the characteristic linear size of the interface. As it is shown in Fig. 2 where four iterations of a fractal interface are given, the linear size of the interface changes rapidly when higher order approximations are taken into account. It is assumed that the opposite sides of the fracture are perfectly matching surfaces, so only one side of the fracture was generated by using the de-

scribed fractal interpolation function. By applying relation (8) the fractal dimension D of the interface studied here results to be equal to 1.369.

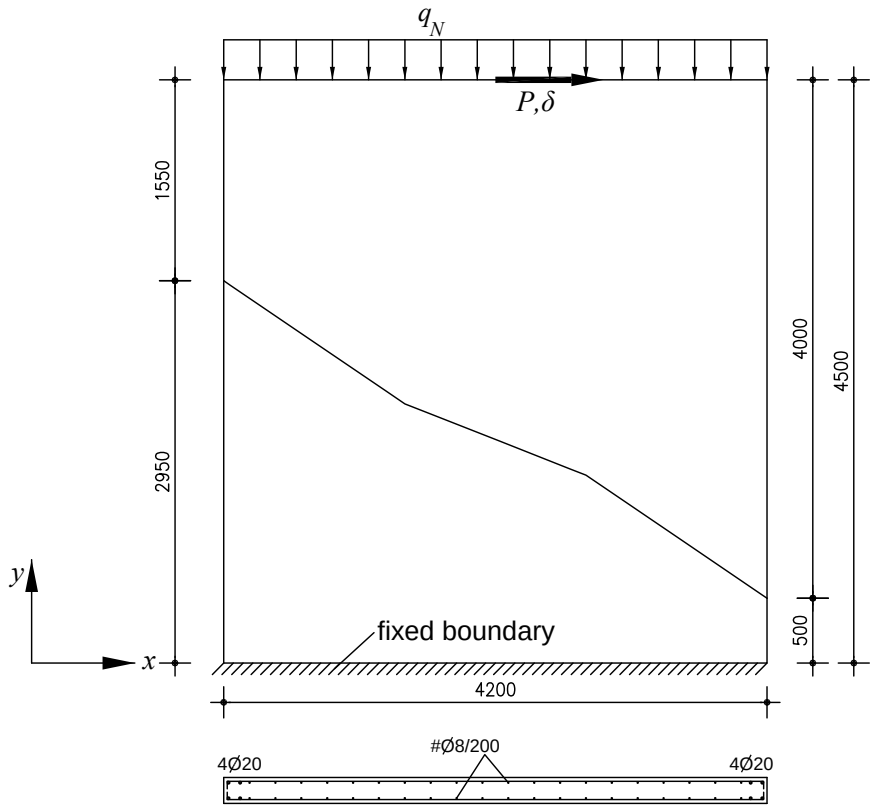

Figure 1: The considered shear wall.

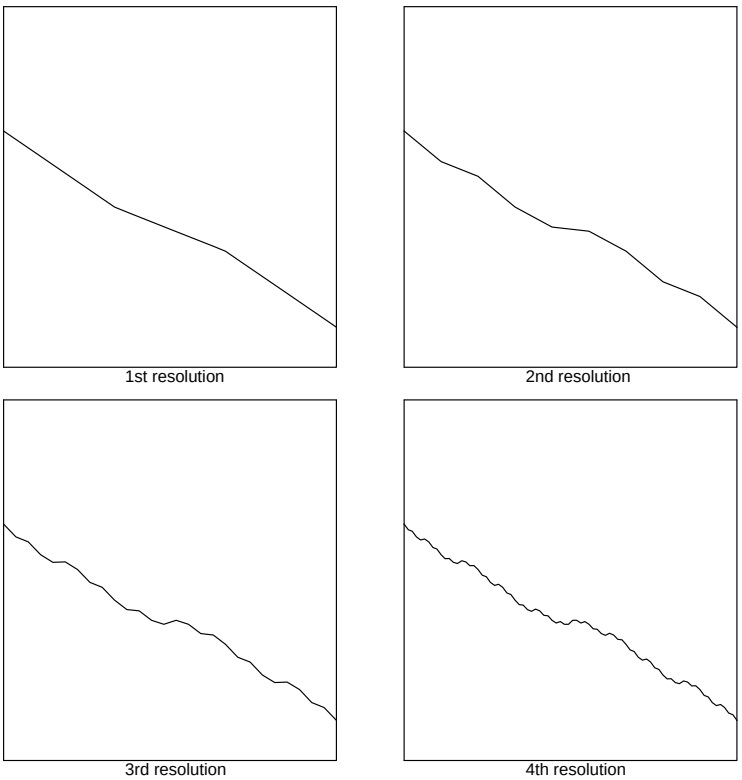

Figure 2: The first four resolutions of the fractal crack.

In Table 1 the characteristics of each resolution are presented. The resolution $\delta^{(n)}$ for each iteration (n) is given in the second column of Table 1. The last column of this table presents the total crack lengths $L^{(n)}$ in m.

Iteration (n)	Resolution $\delta^{(n)}$ (m)	Interface length $L^{(n)}$ (m)
1st	1.404	4.888
2nd	0.468	4.946
3rd	0.156	5.080
4th	0.052	5.373

Table 1: Characteristics of the considered structures

For the modelling of the above problem the finite element method is used. In order to avoid a much more complicated three-dimensional analysis, two-dimensional finite elements were employed, however, special consideration was given to the incorporation of the nonlinearities that govern the response of the wall. More specifically, the mass of the concrete was modelled through quadrilateral and triangular plain stress elements. The finite element discretization density is similar for all the considered problems [19]. This rule ensures that the discretization density will not affect the comparison between the results of the various analyses that were performed.

The modulus of elasticity for the elements representing the mass of concrete was taken equal to $E = 21\,\text{MPa}$ and the Poisson's coefficient equal to $\nu = 0.16$. The material was assumed to follow the nonlinear law depicted in Fig. 3a. Under compression, the material behaves elastoplastically, until a total strain of 0.004. After this strain value crushing develops in the concrete, leading its strength to zero. A more complicated behaviour is considered under tension. More specifically, after the exhaustion of the tension strength of concrete, a softening branch follows, having a slope $k_s = 10^7\,\text{MPa}$. Progressively the tension strength of concrete is also zeroed. The above uni-directional nonlinear law is complemented by an appropriate yield criterion (Tresca) which takes into account the two-dimensional stress fields that develop in the considered problem. For the simulation of cracking a smeared crack algorithm is used, in which the cracks are evenly distributed over the area of each finite element [20].

The steel rebars were modelled through two-dimensional beam elements, which were connected to the same grid of nodes as the plain stress elements simulating the concrete. At each position, the properties that were given to the steel rebars take into account the reinforcement that exists in the whole depth of the wall. For example, the horizontal and vertical elements that simulate the steel mesh are assigned an area of 100.5 mm^2 that corresponds to the cross-sectional area of two 8mm steel rebars. For simplicity, the edge reinforcements were simulated by a single row of beam elements that have an area of 1256mm^2 (i.e. $4\times 314\text{mm}^2$). For the steel rebars, a modulus of elasticity $E = 210\,\text{MPa}$ was assumed. Moreover, the nonlinear laws of Fig. 3b,c were considered for the S220 and S400 steel qualities respectively. These laws exhibit a hardening branch, after the yield stress of the material is attained.

Figure 4 depicts the finite element discretizations for the structures that correspond to the third and fourth iterations of the fractal interface. The grey lines in the finite element meshes correspond to the positions of the steel rebars. The distance between the two facing parts of the interface is only 0.1mm. Special attention was given in the modelling so that the steel rebars retain their initial horizontal and vertical positions, i.e. no eccentricity exists between the corresponding rows of beam finite elements due to the formation of the crack.

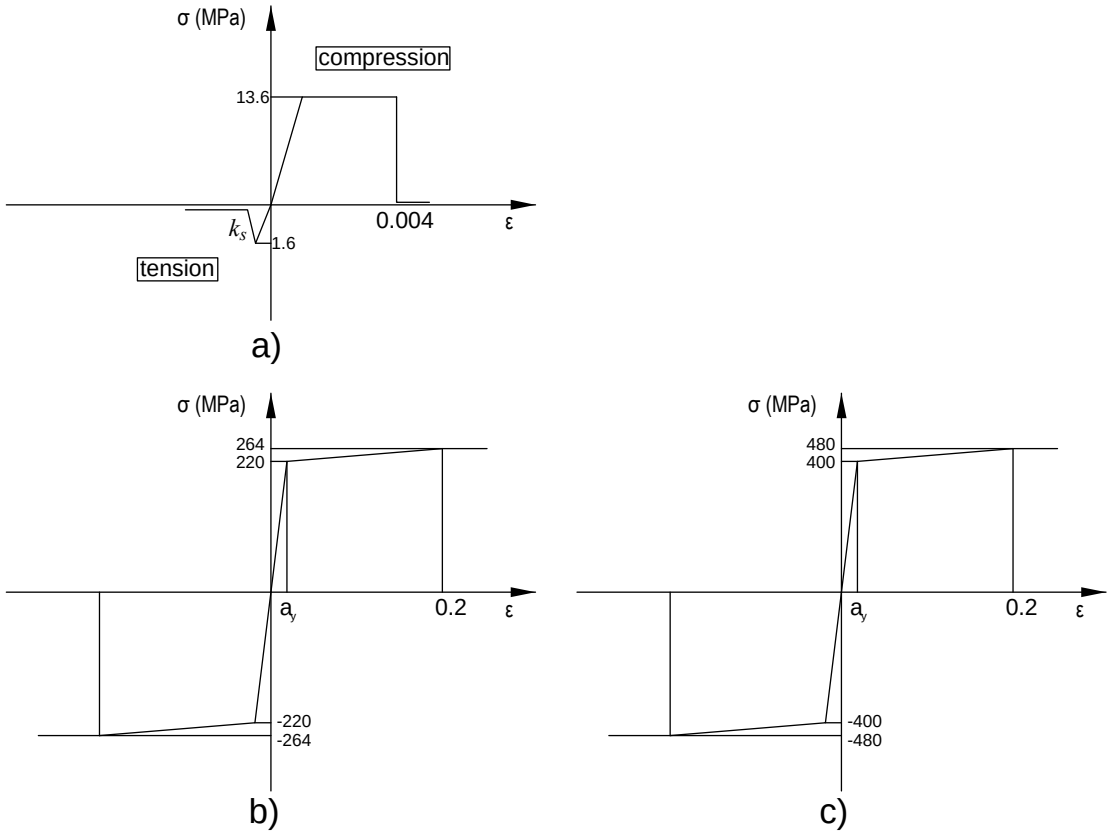

Figure 3: The adopted materials laws a) C16 concrete, b) S220 steel, c) S400 steel.

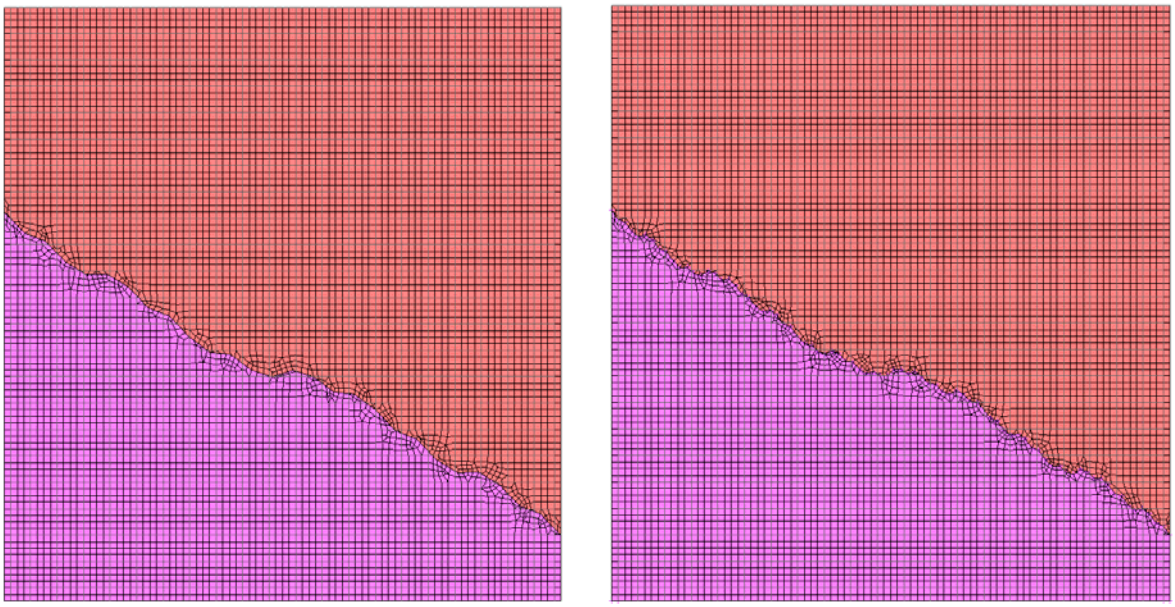

Figure 4: F.E. discretizations for third and fourth approximations of the fractal interface.

In this paper, only the finite element models corresponding to the 3rd and 4th approximations of the fractal crack were considered, because 1st and 2nd approximations don't have meaning from the engineering point of view.

At the interfaces, unilateral contact and friction conditions were assumed to hold. The Coulomb's friction model was followed with a coefficient equal to 0.6 At each scale, where a classical Euclidean problem is solved, a variational formulation [7] was used in order to describe the contact between the two parts of the crack.

For every value of the vertical loading N, a solution is taken in terms of shear forces and horizontal displacements at the interface, for different values of the resolution of the cracked wall and for the case of the uncracked wall. The aim of this work is to study the behaviour of the shear wall, i.e. the behaviour of the concrete and the forces in the rods, as the vertical loading and the resolution of the interface change.

Two cases are considered:

- In the first case the wall is uncracked.
- In the second case, where a fractal crack F has been developed in the wall, different resolutions are taken into account in order to examine how the resolution of a fractal interface F affects the strength of a reinforced concrete shear wall element.

The solution of the above problems is obtained through the application of the Newton-Raphson iterative method. Due to the highly nonlinear nature of the problem, a very fine load incrementation was used. The maximum value of the horizontal displacement (20mm) was applied in 2000 loading steps, while the total vertical loading was applied in the 1st load step and was assumed as constant in the subsequent steps.

4 EXPERIMENTAL AND NUMERICAL RESULTS

Figure 5 presents the applied horizontal load verse the corresponding displacement ($P-\delta$ curves) for the different values of the vertical loading N. It has to be noticed, starting from the case of the uncracked wall, that the value of the vertical loading plays a significant role. As the value of the vertical loading increases, the capacity of the wall to undertake horizontal loading increases as well. However, for the higher load values (for N=2.000 and 2.500 kN), strength degradations are noticed. As it will be explained later, these degradations have their nature to the exhaustion of the shear strength of concrete. However, after this strength degradation, the resistance of the wall increases again as a result of the transfer of the loading from the concrete to the horizontal steel rebars.

Coming now to the cases of the cracked walls, the beneficial effect of the normal compressive loading is once more verified. This result holds for both the 3rd and the 4th approximations of the fractal crack but for small displacement values only. For larger displacement values, the two variants of the cracked wall behave differently. The 4th approximation appears to have a stable behaviour without strength degradations. However, it is noticed that in the case of the 3rd approximation and for heavy axial loading, significant strength degradation takes place.

The above results can be more easily understood if we compare in the same diagram the curves obtained for the three different structures studied here (uncracked, 3rd iteration, 4th itration) for specific load levels. Figure 6 gives the *P-δ* curves for three cases of axial loading, namely for N=0, N=1500kN and N=2.500 kN. It is noticed that for low values of the compressive axial loading, there is actually no difference between the uncracked and the cracked walls. In all the cases the horizontal loading is easily transferred and no signs of strength degradation are noticed. That means that the wall works mainly in bending and the shear forces are well below the shear strength of the wall. For moderate axial loading values (i.e. for N=1.500 kN), it is noticed that the uncracked wall appears to have greater strength that the cracked variants examined here. It is also noticed that the 4th iteration of the fractal crack

leads to greater ultimate strength. This fact can be primarily attributed to the fact that the 4th iteration seems to lead to a greater degree of interlocking between the two parts of the crack.

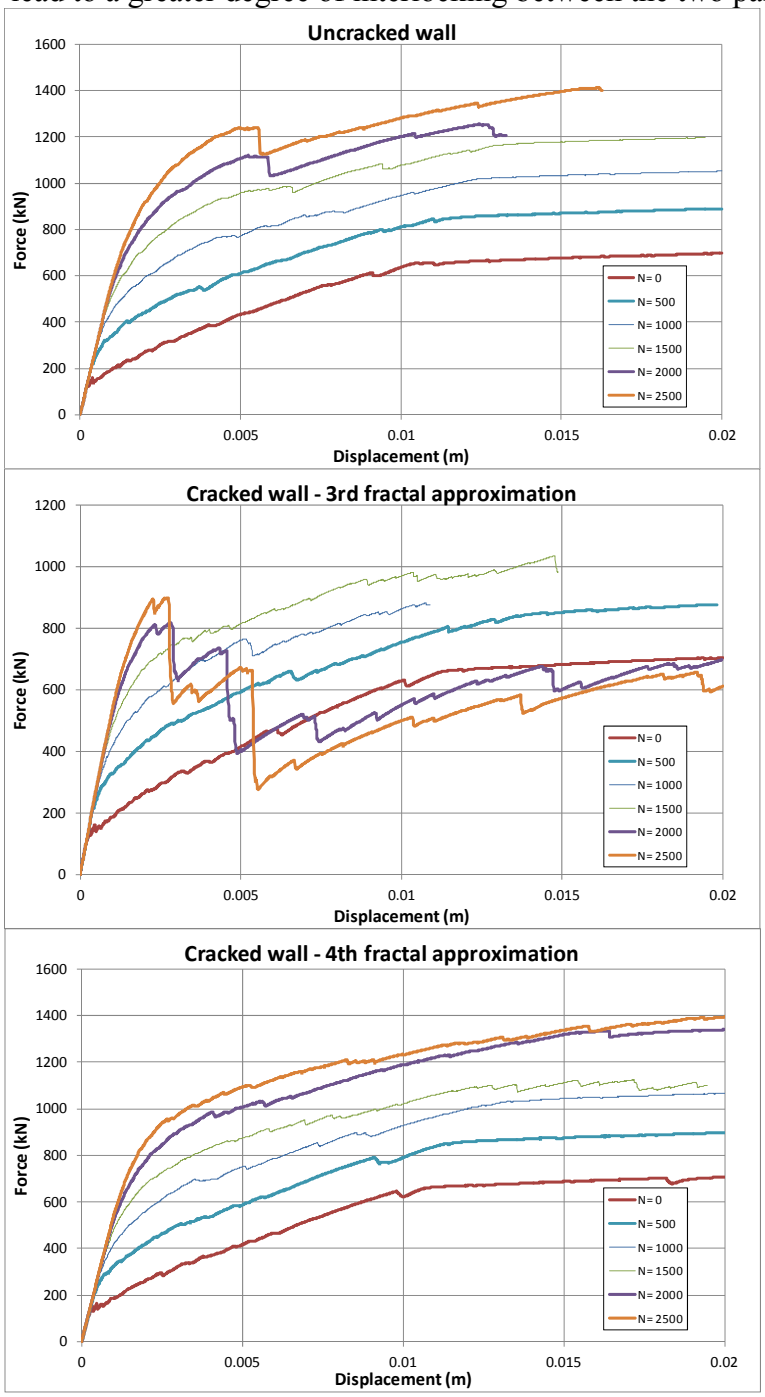

Figure 5: Load-displacement (P-δ) curves for the cases of the uncracked and cracked walls.

However, the most interesting case is that of the heave axial loading (N=2.500 kN). First, it can be noticed that the behavior of the 4th approximation of the fractal crack leads to results that are close enough to those of the uncracked wall. There exist some differences for horizontal displacements in the range of 2-6mm. In this range the uncracked wall exhibit greater resistance. However, for 6mm, the uncracked wall appears strength degradation and after this displacement value the results of the 4th approximation of the fractal crack are again very close to those of the initially uncracked wall.

Significantly different is the case of the 3rd approximation of the fractal crack. It is noticed that although in the first loading steps the results follow closely those of the 4th approximation, after a displacement value of 3mm significant strength degradation appears, having the form of successive vertical branches. The ultimate strength of this wall is significantly lower than the other variants.

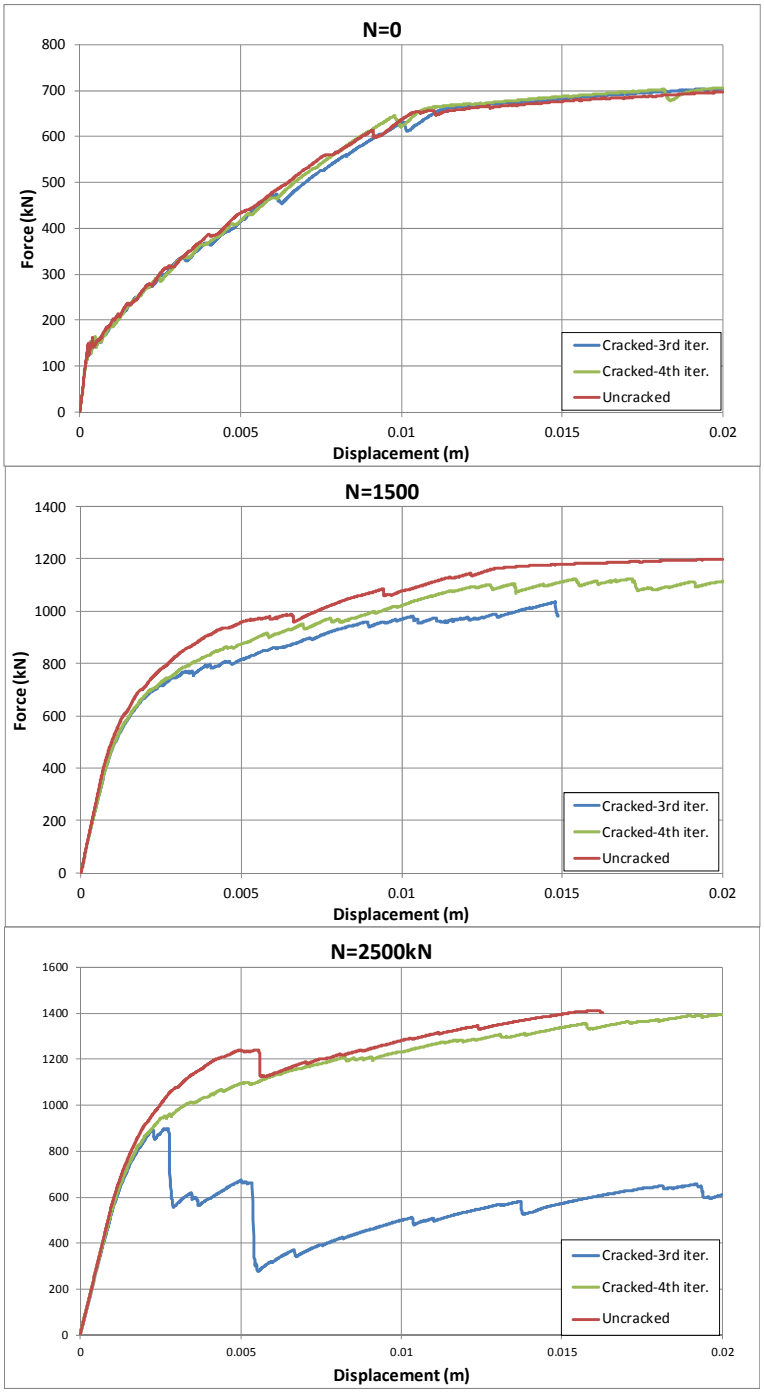

Figure 6: Comparison of the behaviour of the three variants of the examined wall for specific values of the compressive axial loading.

It is interesting to try to explain this significantly different behaviour that appears between the walls corresponding to the 3rd and 4th approximations of the fractal crack. For this reason,

all the parameters affecting the behaviour of the wall will be comparatively studied in the sequel.

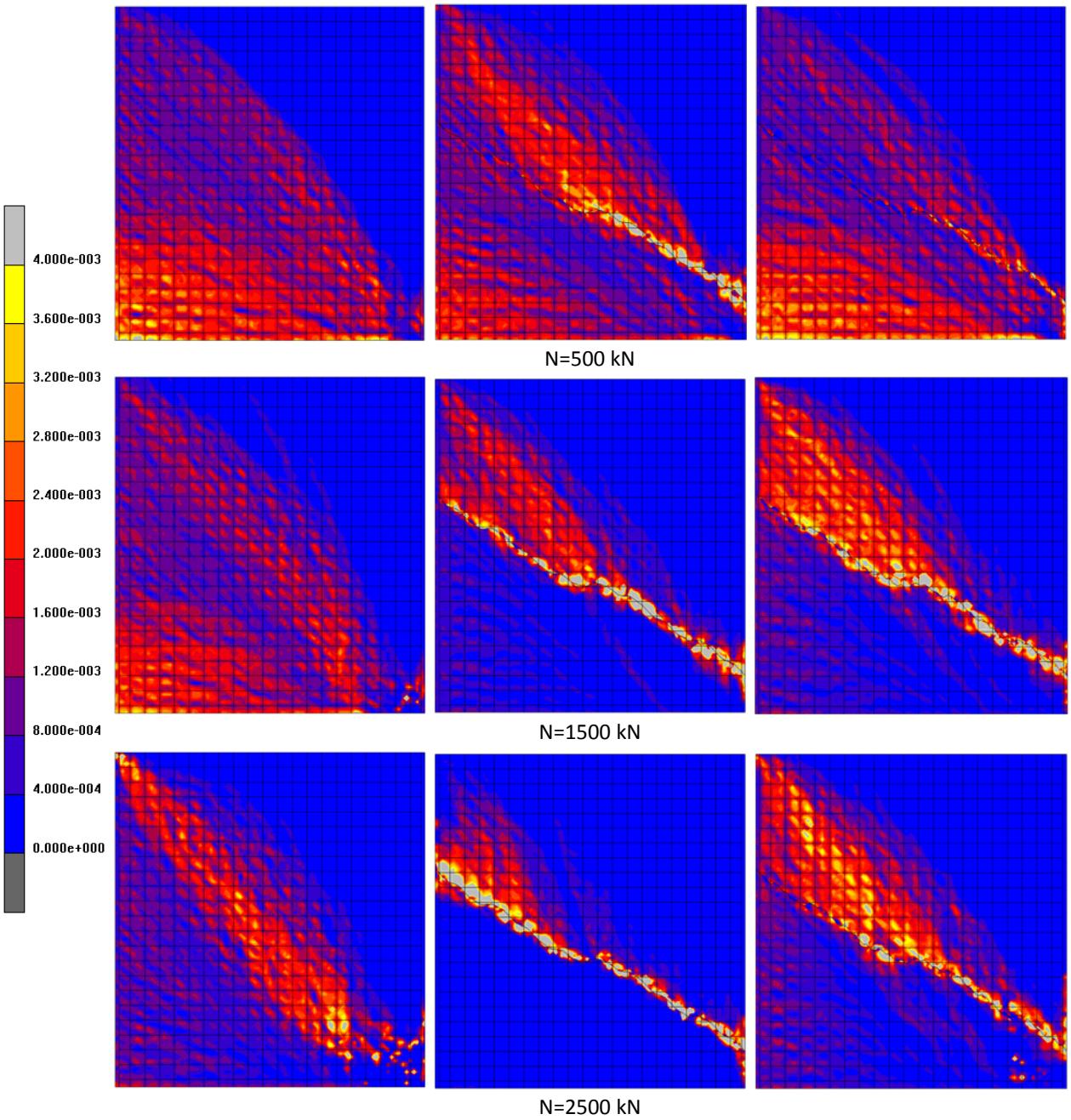

Figure 7: Cracking strains for various values of the vertical loading, for the cases of the uncracked wall (left column) and the cracked walls (3rd approximation- middle column and 4th approximation – right column).

Figure 7 depicts the cracking strains of concrete for specific values of the axial loading. All the depicted results correspond to the end of the analysis, i.e. they have been obtained for an applied horizontal displacement of 20mm. First of all, it can be noticed that for low values of the axial loading, the cracking patterns that have been developed in all the studied walls are rather similar. The larger cracking strain values (yellow and grey colours) have their nature in the bending deformation of the wall. For moderate axial loading, the cracking patterns are quite different. The uncracked wall has again a bending type cracking pattern. The cracked walls seem to behave differently. Both of them exhibit significant cracking in the vicinity of

the crack (grey colors). Apart from this, shear type cracking patterns develop at the upper parts of the walls.

The above results alone cannot explain the significantly different responses that the two cracked variants of the wall exhibit. For this reason, the plastic strains of concrete are examined in the following. Figure 8 depicts the plastic concrete strains for the three different variants of the wall and for specific values of axial loading. The upper value of the presented scale corresponds actually to the crushing limit (grey values). Therefore, it can be considered that the concrete stresses in these areas are actually zero. For the uncracked wall (left column of Fig. 8) it can be noticed that the more heavily deformed region is the lower right corner. It is clear that in this case the wall exhibits a typical bending type deformation behaviour (cracking at the lower left region, crushing at the lower right corner).

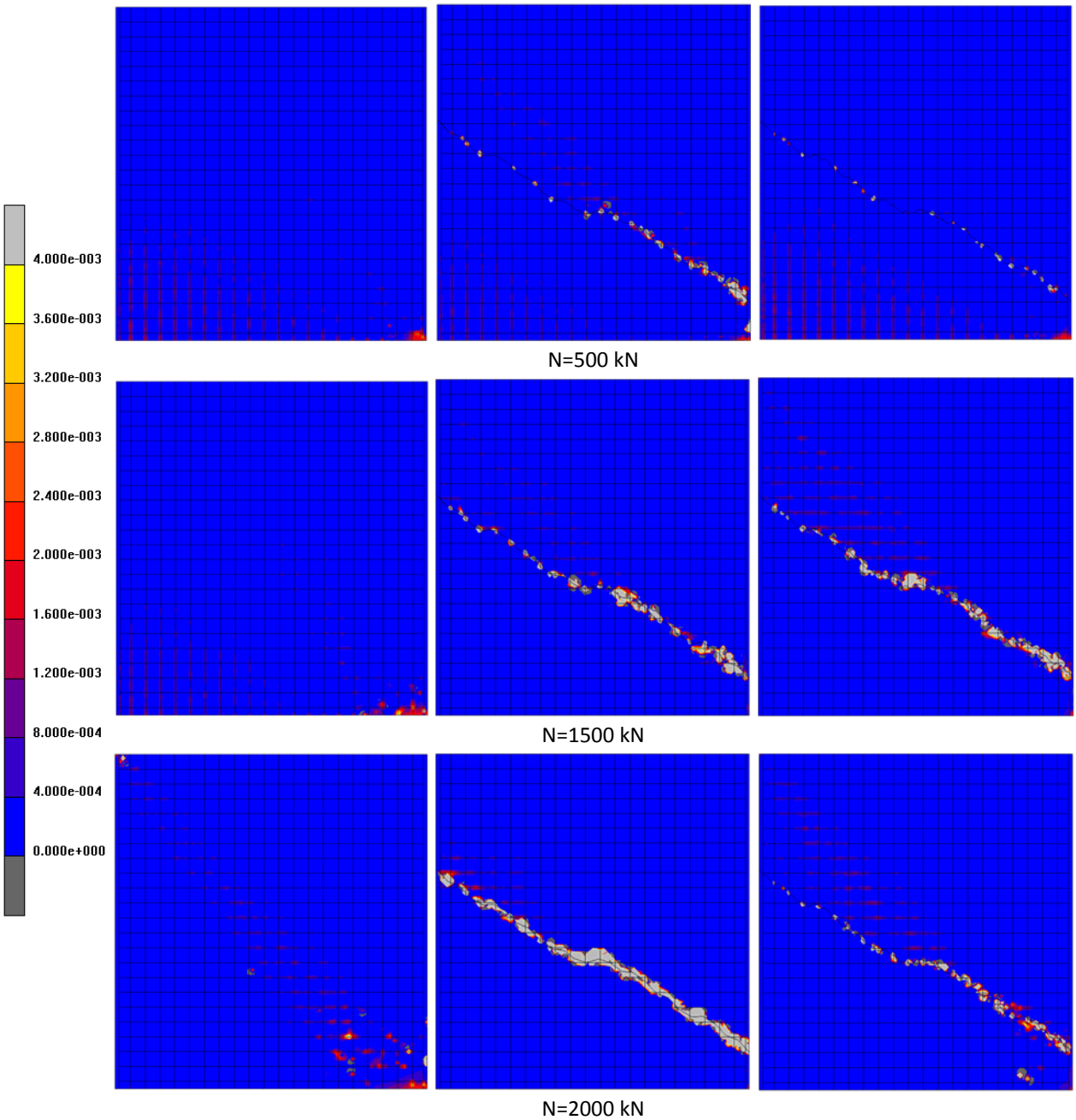

Figure 8: Plastic strains for various values of the vertical loading, for the cases of the uncracked wall (left column) and the cracked walls (3rd approximation- middle column and 4th approximation – right column)

On the other hand, the cracked walls seem to deform significantly in the vicinity of the crack. This phenomenon is more pronounced in the case of the 3rd approximation of the fractal wall. Especially in the case of heavy axial loading, it can be noticed that the vicinity of the crack is in crushed state, i.e. in this region the forces are transmitted solely by the steel mesh (the concrete has no ability to transfer any kind of forces). For the case of the 4th approximation, this phenomenon is rather limited, i.e. it can be concluded that in this case the crack retains partial its ability to transfer shear and compressive forces through the contact and friction phenomena that develop in the interface and through the mechanical interlocking that occurs between the two interface parts.

It is now interesting to examine the deformations that have occurred at the steel mesh. Figure 9 displays the steel mesh for the three variants of the considered wall and for different values of the vertical loading. The presented deformations correspond to the last load step and have been magnified by a factor of 10 so that the differences between the examined cases visible.

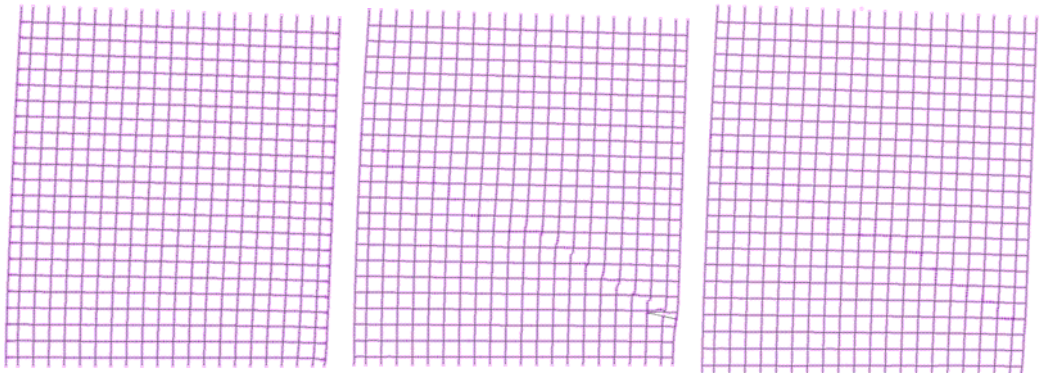

N=500 kN

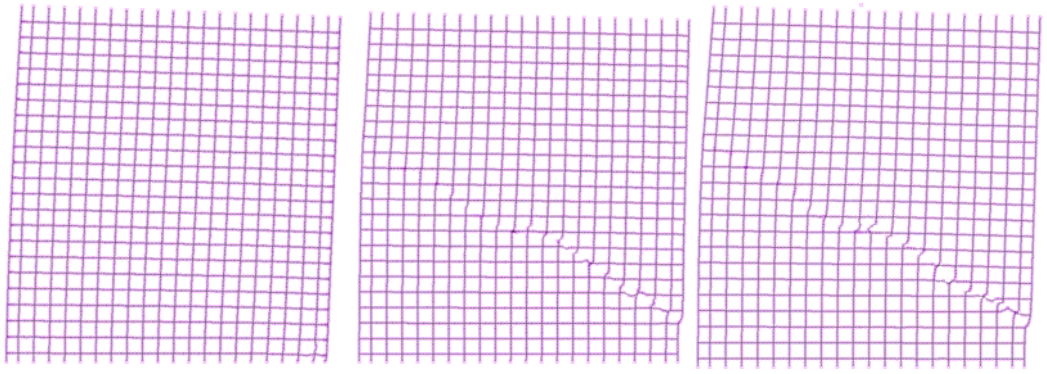

N=1500 kN

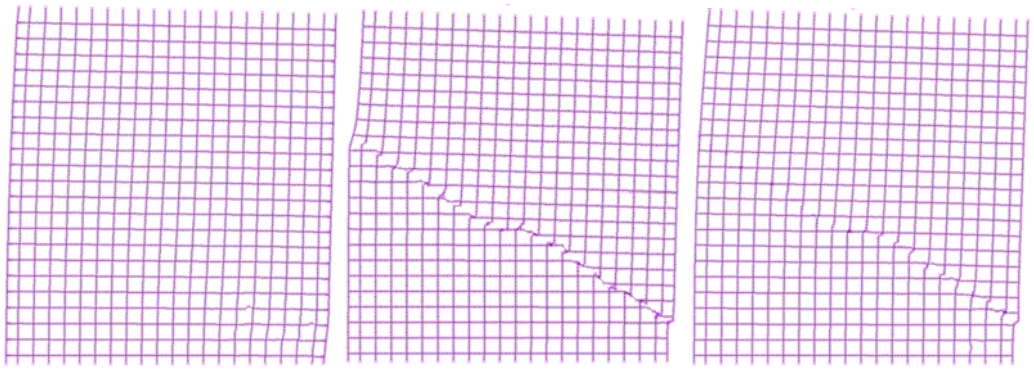

N=2500 kN

Figure 9: Deformation of the steel mesh for various values of the vertical loading, for the cases of the uncracked wall (left column) and the cracked walls (3rd approximation- middle column and 4th approximation – right column).

For low vertical loading values, the deformations of the steel meshes are actually very similar. However, for moderate values of the vertical loading (N=1.000kN) there exist some differences. The steel meshes of the cracked walls seem to be distorted in the vicinity of the right part of the formed crack. In this region the vertical rebars above and below the crack present an offset which can be attributed to the inability of the interface to transfer shear forces. For the case of heavy vertical loading, the situation is different again. The wall corresponding to the 4^{th} resolution of the fractal crack has a deformation similar to that of the case of the moderate loading. However, the steel mesh of the wall corresponding to the 3^{rd} resolution of the fractal crack exhibits significant deformations all along the crack. All the upper vertical rebars present a significant horizontal offset with respect to the lower ones. This horizontal offset is obvious even in the leftmost part of the wall. Moreover, the horizontal rebars of the upper part present a vertical offset with respect to the ones of the lower part. This deformation pattern verifies the findings that were noticed in Fig. 8 concerning the excessive strains in the vicinity of the crack (which had values well above the crushing strain limit). This deformation type of the steel mesh has its nature to the inability of the concrete to transfer any loading in this case.

In the sequel, the difference in the response between the 3^{rd} and the 4^{th} approximations of the fractal crack for the case of the heavy vertical loading will be explained. First of all, it has to be noticed that the higher vertical loading leads also to higher values of the horizontal loading, as it has been explained for the case of the uncracked wall. These increased horizontal forces have to be transferred from the upper part of the cracked wall to its lower part. In this respect, three mechanisms develop in order to facilitate the horizontal load transfer:

- Exploitation of the tensile strength of the horizontal rebars;
- Development of friction on the part of the crack where contact forces occur;
- Mechanical interlock between the two faces of the crack.

The first two mechanisms are almost similar in both cracked walls. However, it is obvious from Fig. 6 that the higher resolution approximations of the fractal crack have improved capacity to transfer forces through the mechanical interlock mechanism. To the authors' opinion, this is the most important reason for the difference in the response between the walls corresponding to the 3^{rd} and the 4^{th} approximation of the fractal crack. For lower vertical load values the differences are rather limited, however, as the vertical loading increases, the response is completely different because the increased vertical forces are combined with the increased horizontal forces and "destroy" completely the vicinity of the interface.

Figures 10,11 and 12 display the forces that develop at the horizontal and vertical rebars of the steel mesh for the three variants of the wall examined here (uncracked, 3^{rd} approximation, 4^{th} approximation respectively) for displacements of 5 and 20mm. The left column of each figure corresponds to lower values of the axial loading (N=500kN), the middle column to moderate loading values (N=1500 kN) and the right column to heavy axial loading (N=2.500 kN).

For the case of the uncracked wall (Fig. 10) it is noticed that in the early horizontal loading steps (δ=5mm), only the vertical rebars are significantly loaded. The rebars in the left side of the wall have tensile forces while the rebars in the right side develop compressive forces, as a result of the bending of the wall. For δ=20mm, after the development of cracking in various parts of the initially uncracked wall, the horizontal rebars are also stressed, mainly in the areas

where the corresponding cracks have reduced or zeroed the ability of concrete to transfer shear forces.

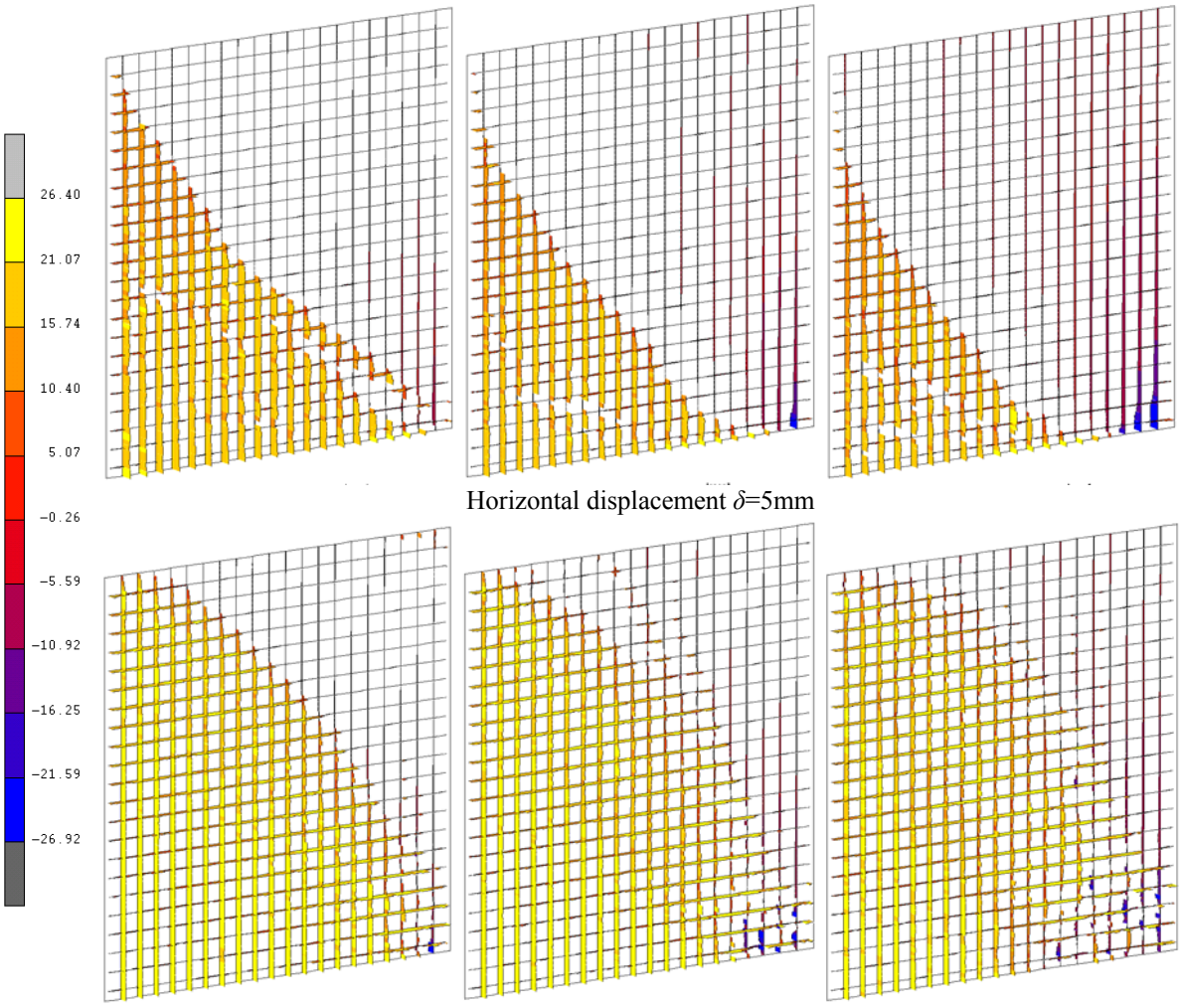

Figure 10: Forces developed in the steel mesh for various values of the vertical loading for the uncracked wall (left column: N=500 kN, middle column: N=1500 kN, right column: N=2500 kN).

For the case of the 3rd approximation of the crack, it is noticed that the vertical rebars are stressed only for small axial loading values. For moderate and heavy axial loading, the vertical rebars are only partial stressed. It deserves to be noticed that the rebar stresses are negative in the vicinity of the crack, a fact that verifies that the concrete is unable to transfer even compressive loading. Moreover, it is noticed that the rebars of the right side of the wall do not develop compressive stresses any more, due to the fact that the magnitude of bending that develops in this case is significantly smaller than that in the case of the uncracked wall. The horizontal rebars are stressed only in specific areas, near the crack and in the regions where cracking strains have been developed. In any case, a closer look in the forces that have been developed in the rebars verifies the significantly decreased bending capacity of the specific wall.

The situation is rather different for the case of the 4th approximation of the fractal crack. The corresponding rebar forces are depicted in Fig. 12. It can easily be verified that for small values of the axial loading, the picture of the forces of the vertical rebars is quite similar to that of the uncracked wall. The same holds also for the forces of the horizontal rebars. For moderate axial load values, the forces of the vertical rebars appear discontinuities. At the right

part of the crack it can be noticed that in some rebars the forces are compressive, indicating again the partial inability of the concrete in this region to transfer compressive loading. The horizontal rebars are mainly stressed in the upper part of the cracked wall and in the vicinity of the crack. Notice that this result is absolutely compatible with the remarks given for the cracked areas in Fig. 7.

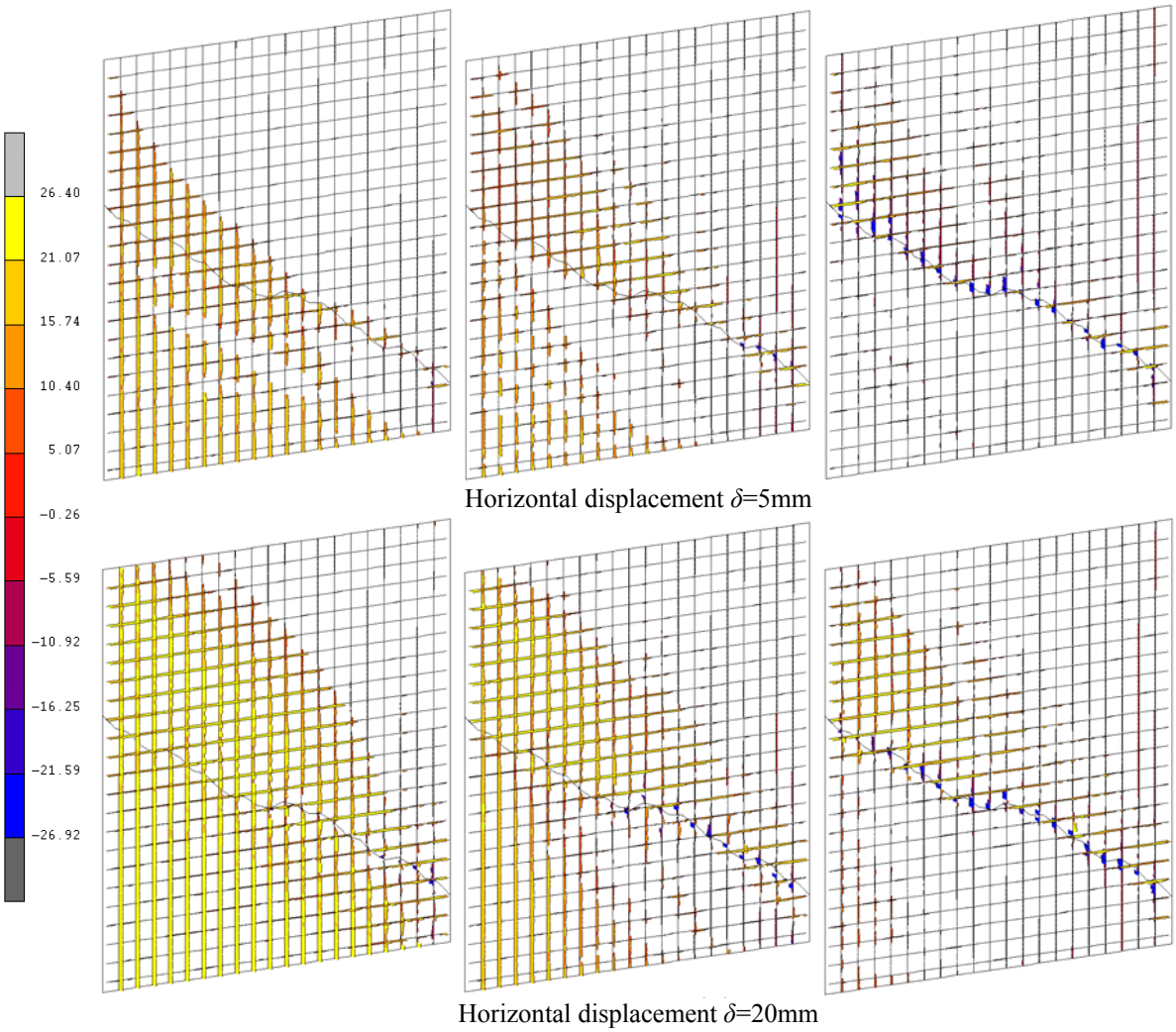

Figure 11: Forces developed in the steel mesh for various values of the vertical loading for the 3rd approximation (left column: N=500 kN, middle column: N=1500 kN, right column: N=2500 kN).

5 CONCLUSIONS

In the paper, the finite element analysis of a typical wall element was presented assuming that a certain crack has been developed as a result of an earthquake action. The crack was modelled following tools from the theory of fractals. Two different resolutions of the fractal curve were considered and their results were compared to those of the initially uncracked wall. The main finding of the paper is that the cracked wall still has the capacity to sustain monotonic horizontal loading. For small axial loading values, this capacity is similar to that of the initially uncracked wall. However, for larger axial loading values, the demands increase. In this case, it seems that a more accurate modelling of the fractal crack (i.e. considering higher values of the resolution) leads to better result. Using lower resolution values, the mechanical interlock between the two faces of the crack is rather limited, leading the concrete in vicinity

of the crack to overstressing and gradually to a complete loss of its capacity to sustain any kind of forces. In this case the bending capacity of the wall is significantly limited with respect to that of the uncracked concrete.

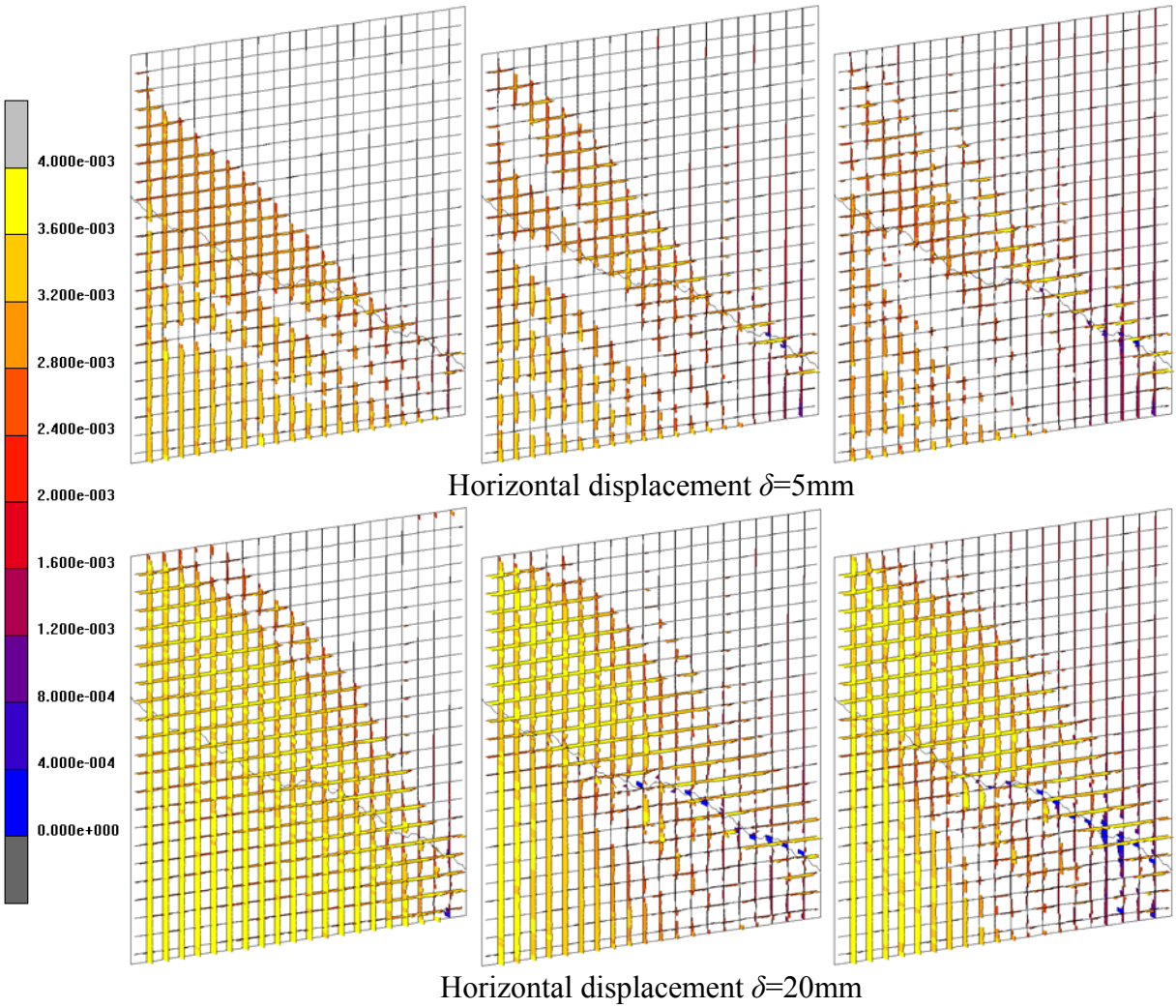

Figure 12: Forces developed in the steel mesh for various values of the vertical loading for the 4th approximation (left column: N=500 kN, middle column: N=1500 kN, right column: N=2500 kN).

REFERENCES

[1] B. Mandelbrot, D. Passoja, A. Paullay, Fractal character of fractured surfaces of metals. *Nature*, **308**, 721-723, 1984.

[2] V.C.B. Saouma, C. Barton, N. Gamaleldin, Fractal characterization of fracture surfaces in concrete. *Eng. Fract. Mech*., **35**, 47-53, 1990.

[3] F.M. Borodich, A.B. Mosolov, Fractal roufhness in contact problems. *Journal of Applied Mathematics and Mechanics*, **56**, 681-690, 1992.

[4] A. Majumdar, C.L. Tien, Fractal characterization and simulation of roufh surfaces, *Wear*, **136**, 313-327, 1990.

[5] Borri-Brunetto, M., Carpinteri, A., and Chiaia, B. (1999), "Scaling phenomena due to fractal contact in concrete and rock fractures", *Int. J. Fracture,* **95**, 221-238, 1999.

[6] O. K. Panagouli, E.S. Mistakidis, Dependence of contact area on the resolution of fractal interfaces in elastic and inelastic problems, *Engineering Computations*, 2010 (in press).

[7] E. Mistakidis and G. Stavroulakis, Nonconvex optimization in Mechanics. Algorithms, heuristic and engineering applications by the FEM, Kluwer, Boston, 1997.

[8] G. Mourot, S. Morel, E. Bouchaud and G. Valentin, "Anomalous scaling of mortar fracture surfaces, *Phys Rev E*, **71**, 2005.

[9] A. Carpinteri, B. Chiaia, S. Invernizzi, Three-dimensional fractal analysis of concrete fracture at the meso-level*, Theor Appl Fract Mech*, **31**, 163-172, 1999.

[10] B. Mandelbrot, The Fractal Geometry of Nature, W.H. Freemann & Company, New York, 1982.

[11] Måloy, K.J., Hansen A., Hinrichsen E.L. and Eoux S., "Experimental measurements of the roughness of brittle cracks", *Phys Rev Lett*, **68**, 213-215, 1992.

[12] A. Majumdar, and B. Buhushan, "Role of fractal geometry in roughness characterization and contact mechanics of surfaces", *Trans ASME J. Tribology*, **112**, 205-216, 1990.

[13] P.D. Panagiotopoulos and O.K. Panagouli, "Fractal geometry in contact mechanics and numerical applications", in Carpintieri, A. and Mainardi, F. (Ed.), *CISM-Book on Scaling, Fractals and Fractional Calculus in Continum Mechanics,* Springer Verlag, 109-171, 1997.

[14] F.M. Borodich and D.A. Onishchenko, "Similarity and fractality in the modeling of roufhness by a multilevel profile with hierarchical structure" *Solids and Structures*, **36**(17), 2585-2612.

[15] E.S. Mistakidis and O.K. Panagouli, (2002), "Strength evalution of retrofit shear wall elements with interfaces of fractal geometry", *Engineering Structures*, **24**, 649-659, 2002.

[16] Mistakidis, E.S. and Panagouli, O.K., "Friction evolution as a result of roughness in fractal interfaces", *Engineering Computations*, **20(**1), 40-57, 2003.

[17] Ching-Ju Chen, Tzong-Yeang Lee, Y. M. Huang, and Fu-Jou Lai, "Extraction of characteristic points and its fractal reconstruction for terrain profile data",*Chaos, Solitons& Fractals*, **39,** 1732-1743, 2009.

[18] M. Barnsley, Fractals Everywhere, Academic Press, Boston- New York, 1988.

[19] Hu, Guang-Di, P.D. Panagiotopoulos, O.K. Panagouli, O. Scherf and P. Wriggers, "Adaptive finite element analysis of fractal interfaces in contact problems", *Comp. Methods Appl. Mech. Engrg*., **182,** 17-37, 2000.

[20] R. deBorst, J. Remmers, A. Needleman, and M-A Abellan, "Discrete vs smeared crack models for concrete fracture: bridging the gap", *Int J Numer Anal Met*, **28**(7-8), 583-607, 2004.